# High Prevalence of *Helicobacter* Species Detected in Laboratory Mouse Strains by Multiplex PCR-Denaturing Gradient Gel Electrophoresis and Pyrosequencing

Hans-Olof Nilsson,[1] Ibn-Sina Ouis,[1] Unne Stenram,[2] Åsa Ljungh,[1] Anthony P. Moran,[3] Torkel Wadström,[1] and Waleed Abu Al-Soud[1]*

*Department of Medical Microbiology, Dermatology and Infection[1] and Department of Pathology,[2] Lund University, Lund, Sweden, and Department of Microbiology, National University of Ireland, Galway, Ireland[3]*

**Rodent models have been developed to study the pathogenesis of diseases caused by *Helicobacter pylori*, as well as by other gastric and intestinal *Helicobacter* spp., but some murine enteric *Helicobacter* spp. cause hepatobiliary and intestinal tract diseases in specific inbred strains of laboratory mice. To identify these murine *Helicobacter* spp., we developed an assay based on PCR-denaturing gradient gel electrophoresis and pyrosequencing. Nine strains of mice, maintained in four conventional laboratory animal houses, were assessed for *Helicobacter* sp. carriage. Tissue samples from the liver, stomach, and small intestine, as well as feces and blood, were collected; and all specimens ($n = 210$) were screened by a *Helicobacter* genus-specific PCR. Positive samples were identified to the species level by multiplex denaturing gradient gel electrophoresis, pyrosequencing, and a *H. ganmani*-specific PCR assay. Histologic examination of 30 tissue samples from 18 animals was performed. All mice of eight of the nine strains tested were *Helicobacter* genus positive; *H. bilis*, *H. hepaticus*, *H. typhlonius*, *H. ganmani*, *H. rodentium*, and a *Helicobacter* sp. flexispira-like organism were identified. *Helicobacter* DNA was common in fecal (86%) and gastric tissue (55%) specimens, whereas samples of liver tissue (21%), small intestine tissue (17%), and blood (14%) were less commonly positive. Several mouse strains were colonized with more than one *Helicobacter* spp. Most tissue specimens analyzed showed no signs of inflammation; however, in one strain of mice, hepatitis was diagnosed in livers positive for *H. hepaticus*, and in another strain, gastric colonization by *H. typhlonius* was associated with gastritis. The diagnostic setup developed was efficient at identifying most murine *Helicobacter* spp.**

Mouse models are widely used in biomedical research because of the physiological and genetic similarities of mice with humans, low maintenance costs, and the availability of immunological reagents and a large number of inbred as well as transgenic and knockout strains (20). Moreover, the complete mouse genome has recently been published (http://www.informatics.jax.org/) (21).

The genus *Helicobacter* comprises 24 formally named species and is a group of microaerophilic, gram-negative, spiral to curve-shaped bacteria isolated from the stomachs and intestines of humans and various animal species (8). After the first isolation of *Helicobacter muridarum* from the intestinal mucosa of rats and mice (16), other *Helicobacter* spp., such as *H. hepaticus*, *H. bilis*, *H. rodentium*, *H. typhlonius*, *H. trogontum*, and *H. ganmani*, were isolated from laboratory mice (23, 31). *H. hepaticus* infects the liver and intestinal tract and causes enterocolitis, typhlitis, and hepatitis in germfree mice (7). Furthermore, in susceptible strains (e.g., A/JCr mice), *H. hepaticus* causes chronic hepatitis and hepatocellular carcinoma (5, 29). *H. bilis* colonizes the liver and intestinal tract of mice, has been associated with multifocal chronic hepatitis, and in particular, induces inflammatory bowel disease in interleukin-10-deficient (IL-10$^{-/-}$) mice (3, 6). *H. typhlonius* causes colitis and typhlitis in severe combined immunodeficient (SCID) and IL-10$^{-/-}$

mice (11). *H. rodentium* and *H. ganmani* have been isolated from the mouse intestine, but the pathogenic potentials of these species are unclear (23, 26), although *H. rodentium* has been isolated from a colony of SCID mice with diarrhea coinfected with *H. bilis* (27).

Various methods for the diagnosis of *H. pylori* infections in humans have been developed and evaluated, such as culture, microscopy, urease activity tests, PCR assays, and serology (2). For other helicobacters, detection depends on culture, and PCR assays were developed for some species (12, 24). Conventional culturing for the detection of *Helicobacter* spp. is time-consuming, up to 3 weeks of culture may be necessary for biochemical and phenotypic characterization of some species, and many enteric species are difficult to culture (24). In addition, the presence of a growing numbers of *Helicobacter* spp. in several animal hosts as well as humans precludes species-specific PCR assays for detection.

The 16S ribosomal DNA (rDNA) consists of highly conserved and highly variable regions (4). Denaturing gradient gel electrophoresis (DGGE) of 16S rDNA has previously been used to identify total microbial populations or groups of bacteria in activated sludge and soil, to analyze seasonal changes of marine bacterial communities and the bacterial compositions of different biofilms, and to study the affiliations of the predominant bacteria in human feces (19). In our laboratory, PCR-DGGE was previously optimized to detect and identify various *Helicobacter* spp. (1). Recently, pyrosequencing successfully identified *Helicobacter* spp. and other bacteria,

* Corresponding author. Mailing address: Department of Medical Microbiology, Dermatology and Infection, Lund University, Sölvegatan 23, SE-223 62 Lund, Sweden. Phone: 46 46 173298. Fax: 46 46 189117. E-mail: abu.al-soud@mmb.lu.se.

based on sequencing of short segments of the 16S rDNA (15, 18).

The aim of this study was to further increase the efficiency of PCR-DGGE by analyzing two regions of the *Helicobacter* 16S rDNA (the V3 and V6-7 regions), followed by pyrosequencing of the V3 region. The efficiency of the optimized method was evaluated with gastric, intestinal, and hepatic murine tissue specimens in order to study the distribution of *Helicobacter* spp. and their association with disease, as determined by histopathological analysis of tissue samples.

## MATERIALS AND METHODS

**Bacterial strains.** The murine reference *Helicobacter* strains, obtained from the Culture Collection of the University of Gothenburg (CCUG), Gothenburg, Sweden, included in this study were *H. pylori* (CCUG 17874), *H. bilis* (CCUG 38995, CCUG 41387), *H. ganmani* (CCUG 43527), *H. hepaticus* (CCUG 44777, CCUG 33637), *H. muridarum* (CCUG 29262), and *Helicobacter* sp. flexispira taxon 8 (CCUG 23435). Additional strains were *H. rodentium* 1707, 2060, and 2178; *H. trogontum* MIT 955.369.9136; and *H. muridarum* ST2. The strains were cultured on brucella blood agar supplemented with 0.1% activated charcoal, as described previously (28), in an atmosphere-generating Anoxomat WS 9000 apparatus (Mart Microbiology, Lichtenvoorde, The Netherlands) at 37°C under microaerobic conditions for all strains except *H. ganmani*, which was cultured anaerobically.

**Animals.** The mouse strains used in this study were obtained from four different laboratory animal houses (animal houses AH-1 to AH-4). All mice ($n = 42$ mice, with 22 females) were 15 to 26 weeks of age (mean age, 19 weeks). The mouse strains analyzed were as follows: from AH-1, C57BL/6 mice (three females and three males); from AH-2, specific-pathogen-free (SPF) and SCID (SPF-SCID) mice (five females), SCID mice (two males), and B6sJ1 mice (three females); from AH-3, BALB/cA mice (five males), C3H/HeJ mice (four males), C57BL/6 mice (six females), and C57BL/6 Apo-E$^{-/-}$ mice (five females); and from AH-4, C57BL/6 IL-10$^{-/-}$ mice (six females). All animals were housed conventionally and were fed a standard diet and water ad libitum (7). All mice were euthanized by exposure to $CO_2$; and tissue samples were taken from the liver, stomach, and small intestine. Feces and blood were also collected from each animal. The specimens were flash frozen in liquid nitrogen and stored at −80°C. All mice were treated according to a protocol (permit no. M264-02) approved by the Animal Ethics Research Committee at Lund University.

**DNA extraction.** DNA was extracted from bacteria with a QIAamp DNA Mini kit (Qiagen, Hilden, Germany) or an Easy-DNA kit (Invitrogen Corporation, Carlsbad, Calif.) and from specimens of liver, stomach, small intestine, and blood with the QIAamp DNA Mini kit (Qiagen). All samples were extracted according to the instructions of the manufacturers. Approximately $10^8$ CFU of each bacterial strain, 20 mg of each tissue sample, or 80 μl of blood was incubated overnight with 20 μl of proteinase K solution and 180 μl of extraction buffer. After digestion the DNA was purified on affinity columns provided with the kits. Fecal samples (200 mg) were extracted with a QIAamp DNA Stool Mini kit (Qiagen), according to the instructions of the manufacturer. The purified DNA samples were frozen at −20°C.

**PCR analysis.** Amplification was carried out with a GeneAmp 2700 Thermocycler (Applied Biosystems, Foster City, Calif.). The reaction mixture of the first step (25 μl) contained 0.5 μM each primers C97 and C05 (9), 0.8 mM deoxynucleoside triphosphates (Amersham Biosciences, Uppsala, Sweden), 1× chelating buffer, 2.5 mM MgCl$_2$, 0.4% (wt/vol) bovine serum albumin, 1.25 U of rTth DNA polymerase (Applied Biosystems), and 5 μl of extracted DNA. The amplification conditions for the first step were 94°C for 4 min; 30 cycles of 94°C for 1 min, 50°C for 1 min, and 72°C for 2 min; and finally, 72°C for 5 min. Amplification of the V3 region was done in a 25-μl reaction mixture containing 0.5 μM modified primers BSF917 (5′-GAATAGACGGGG ACCC-3′) and BSR1114 with a GC clamp (5′-CGCCCGCCGCGCCCCGCGCCCGTCCCGCCGCCCC CGCCCGGGGGTTGCGCTCGTTGC-3′) (http://rrna.uia.ac.be/primers), 0.8 mM deoxynucleoside triphosphates (Amersham Biosciences), 1× buffer II, 2.5 mM MgCl$_2$, 1.0 U of AmpliTaq Gold DNA polymerase (Applied Biosystems), and 2 μl of the PCR product from the first step diluted 10 times. The amplification conditions for the V3 PCR were 94°C for 10 min; 35 cycles of 94°C for 30 s, 50°C for 30 s, and 72°C for 30 s; and finally, 72°C for 5 min. Amplification of the V6-7 region was performed as described elsewhere (1). As a positive control, 0.1 ng of *H. pylori* (CCUG 17874) DNA was added to the reaction mixture, whereas 5 μl of sterile deionized water filtered through a Millipore (Bedford, Mass.) filter was

used as a negative control. Detection of the amplified PCR products was done by agarose gel electrophoresis (1).

**DGGE.** The 16S rDNA sequences of different *Helicobacter* spp. were analyzed with WinMelt software (Bio-Rad, Hercules, Calif.) to assist with primer selection and to determine DGGE conditions. DGGE analysis of the V3 region (15 μl) was performed on 9% polyacrylamide (acrylamide-bisacrylamide [37.5:1]) gels containing a urea and formamide gradient from 20 to 40% (100% denaturing solution contained 7 M urea and 40% [vol/vol] formamide). DGGE analysis of the V6-7 region (15 μl) was performed as described previously (1). Electrophoresis was performed at 60°C in 0.5× TAE buffer (20 mM Tris, 10 mM acetic acid, 0.5 mM EDTA [pH 8.3]) at 200 V for 4 h with a DCode electrophoresis unit (Bio-Rad). The gels were stained with ethidium bromide (0.2 μg/ml in 0.5× TAE buffer) for 15 min and visualized with a GelFotoStation (Techtum Lab, Umeå, Sweden).

**Pyrosequencing of the V3 region.** The separated DNA fragments were excised from DGGE gels with a scalpel and transferred to microcentrifuge tubes containing 160 μl of sterile deionized water filtered through a Millipore filter. To separate the DNA from the polyacrylamide gel, the tubes were briefly centrifuged (6,000 × g, 10 s) and subjected to two freeze-thaw cycles (−80°C for 1 h, room temperature for 1 h, and −80°C for 1 h). Subsequently, the specimens were thawed at 4°C for 2 h and 2.0 μl was used as a template in a PCR mixture containing biotinylated primers BSF917 and BSR1114 under the conditions described above. *Helicobacter* genus-specific PCR products were purified from the agarose gels with Ultrafree DA centrifuge tubes (Millipore). Single-stranded DNA was obtained with a Vacuum Prep workstation (Pyrosequencing AB, Uppsala, Sweden). Streptavidin-coated Sepharose beads (Amersham Biosciences) were added to the PCR plate containing the biotinylated PCR products, and the mixture was agitated (10 min, room temperature). A vacuum was applied, and the beads with immobilized PCR products were moved to a separate trough, where 70% (vol/vol) ethanol was aspirated through the filter probes. The Prep Tool of the workstation was then placed in a trough of 0.5 M sodium hydroxide to denature and release the single-stranded DNA while 5′ biotinylated strands remained immobilized on the beads. Next, the beads were washed (10 mM Tris-acetate buffer [pH 7.6]) and transferred to a 96-well pyrosequencing plate containing 1× annealing buffer (20 mM Tris-acetate, 2 mM magnesium acetate tetrahydrate [pH 7.6]) and sequencing primer (GCGAAGAACCTTACC). With the vacuum pressure switched off, a gentle shake of the Prep Tool released the beads into the pyrosequencing plate, which was heated (80°C, 5 min) and left to cool at room temperature to allow annealing of the sequencing primer. The pyrosequencing plate was placed into the process chamber of a PSQ 96 (Pyrosequencing AB) instrument. Enzymes, substrates, and nucleotides from the PSQ 96 SQA reagent kit (Pyrosequencing AB) were dispensed. The nucleotide dispensing order was TCAGCTGACATGATGAGAGATCTCTAGATGAGTCG AGTGTCTAGTCTCTGAG-10(ACTG). A charge-coupled device camera registered the light emitted from each incorporated nucleotide. Analysis of pyrograms was performed with pyrosequencing (version 2.0) software (Pyrosequencing AB), and sequence data were subjected to the BLAST sequence homology search program (http://www.ncbi.nlm.nih.gov/).

**Sanger sequencing.** The separated PCR products of the V6-7 region were excised from the DGGE gels with a scalpel and transferred to microcentrifuge tubes containing 160 μl of sterile deionized water filtered through a Millipore filter. DNA sequencing of the PCR products was carried out as described earlier (1). The closest known relatives of the partial 16S rDNA sequences were determined by using the BLASTN (version 2.2.1) algorithm (http://www.ncbi.nlm.nih .gov/BLAST/).

***H. ganmani*-specific PCR.** Discrimination between *H. ganmani* and *H. rodentium* was performed by a *H. ganmani*-specific PCR assay targeting the 16S to 23S rDNA internal spacer region (28a). Briefly, DNA extracted from mouse specimens that generated genus-specific PCR products similar to those of *H. ganmani* and *H. rodentium*, as determined by DGGE, were amplified with forward primer Gan-F (5′-CTCCTAAGCCCACCAGAAATTG-3′) and reverse primer 16-23SR (5′-CTTATCGCAGTCTAGTACG-3′) in the first step and primers Gan-F and Gan-R (5′-TTCCCCATAATAGGGTAGTTTA-3′) in the second step. The amplification conditions for the first and second steps were 94°C for 2 min, followed by 30 cycles of 30 s each at 94, 48, and 72°C and a final extension at 72°C for 7 min.

**Histologic examination.** *H. hepaticus* and *H. typhlonius* have previously been shown to cause pathological changes in specific strains of deficient mice (7, 11). On the basis of the identification results obtained in this study, 30 tissue biopsy specimens from 18 animals, comprising mainly liver tissue ($n = 15$), stomach tissue ($n = 12$), and some intestinal tissue ($n = 3$) samples, either negative for *Helicobacter* spp. by PCR ($n = 9$) or colonized with *H. hepaticus* ($n = 10$) or *H. typhlonius* ($n = 11$), were fixed in 4% neutral buffered formaldehyde and

TABLE 1. Prevalence of *Helicobacter* spp. in conventional mice determined by *Helicobacter* genus-specific PCR analysis

| Animal house | Mouse strain | No. of mice positive/total no. of mice tested | | | | | |
| --- | --- | --- | --- | --- | --- | --- | --- |
| | | Feces | Stomach | Liver | Small intestine | Blood | Total |
| AH-1 | C57BL/6 | 6/6 | 3/6 | 0/6 | 1/6 | 0/6 | 10/30 |
| AH-2 | SPF-SCID | 5/5 | 3/5 | 4/5 | 1/5 | 3/5 | 16/25 |
| AH-2 | B6sJl | 3/3 | 2/3 | 1/3 | 0/3 | 0/3 | 6/15 |
| AH-2 | SCID | 2/2 | 1/2 | 0/2 | 1/2 | 2/2 | 6/10 |
| AH-3 | BALB/cA | 5/5 | 4/5 | 3/5 | 2/5 | 1/5 | 15/25 |
| AH-3 | C57BL/6 | 6/6 | 3/6 | 0/6 | 1/6 | 0/6 | 10/30 |
| AH-3 | C3H/HeJ | 4/4 | 3/4 | 0/4 | 1/4 | 0/4 | 8/20 |
| AH-3 | ApoE$^{-/-}$ | 5/5 | 4/5 | 1/5 | 0/5 | 0/5 | 10/25 |
| AH-4 | IL-10$^{-/-}$ | 0/6 | 0/6 | 0/6 | 0/6 | 0/6 | 0/30 |
| Total | | 36/42 | 23/42 | 9/42 | 7/42 | 6/42 | 81/210 |

embedded in paraffin by standard methods. Embedded samples were sectioned at 5-$\mu$m thickness and stained with hematoxylin-eosin. The sections were examined by light microscopy for evidence of histopathologic changes.

## RESULTS

**PCR detection of *Helicobacter* spp. in mice.** The distribution of *Helicobacter*-positive samples among the different mouse strains is shown in Table 1. The *Helicobacter* genus-specific PCR assay detected *Helicobacter* DNA in at least one of the five specimens sampled from each mouse, i.e., in 81 of 210 (38.6%) of the specimens examined and in 36 of 42 (85.7%) of the mice analyzed. All animals except for the six IL-10$^{-/-}$ mice from AH-4 were PCR positive for *Helicobacter* in feces; all samples from the IL-10$^{-/-}$ mice tested were *Helicobacter* negative. Gastric tissue samples from 23 of 42 (54.8%) animals were positive. The lowest prevalence of helicobacter was observed in blood samples (6 of 42 [14.3%]), followed by those from the small intestine (7 of 42 [16.7%]) and then those from the liver (9 of 42 [21.4%]). *Helicobacter* DNA was equally distributed in gastric and intestinal tissue specimens, regardless

of the mouse strain and source (i.e., animal house). However, a strain-dependent *Helicobacter* prevalence was observed in liver tissue and blood samples (Table 1). For liver tissue samples, 80% (4 of 5) of the SPF-SCID mice from AH-2 and 60% (3 of 5) of the BALB/cA mice from AH-3 were *Helicobacter* positive, whereas liver samples from only 2 of the remaining 32 animals were *Helicobacter* positive. *Helicobacter* DNA was detected in the blood of five of seven (71%) SCID mice (conventional SCID mice plus SPF-SCID mice), whereas the blood of only one additional mouse was positive. The prevalence of *Helicobacter* sp. DNA among the different mouse strains was highest in the SPF-SCID strain of mice (16 of 25 mice [64%]), followed by conventional SCID mice (6 of 10 [60%]) and BALB/cA mice (15 of 25 [60%]). The rates of detection of *Helicobacter* spp. in specimens of the remaining mouse strains ranged from 0 to 40%. A similar prevalence was observed in C57BL/6 mice, which were collected from two animal houses (AH-1 and AH-3) (Table 1).

**PCR-DGGE and pyrosequencing analysis.** The principle of the diagnostic assay developed in this study is shown in Fig. 1. PCR-DGGE analysis of the V3 and V6-7 regions was efficient at identifying murine *Helicobacter* spp. by defining a specific mobility pattern of the PCR product for each species except *H. ganmani* and *H. rodentium*, whose amplicons could not be differentiated on the DGGE gels (Fig. 2 and Table 2). Therefore, an *H. ganmani*-specific PCR assay was applied to specimens with PCR products that migrated similar to those of *H. ganmani* and *H. rodentium* in the DGGE analysis (Table 2). DGGE detected 94 PCR products from 81 PCR-positive specimens, due to the presence of more than one PCR product in some samples with different DGGE profiles. DGGE of the V6-7 region of the PCR products amplified from specimens from mice in AH-2 and AH-3 showed migration patterns different from those of the other murine *Helicobacter* type strains tested (Fig. 2), whereas DGGE of the V3 region showed a migration pattern similar to that for *H. muridarum* for 38 of 84 (45%) of *Helicobacter*-positive specimens. BLAST analysis of

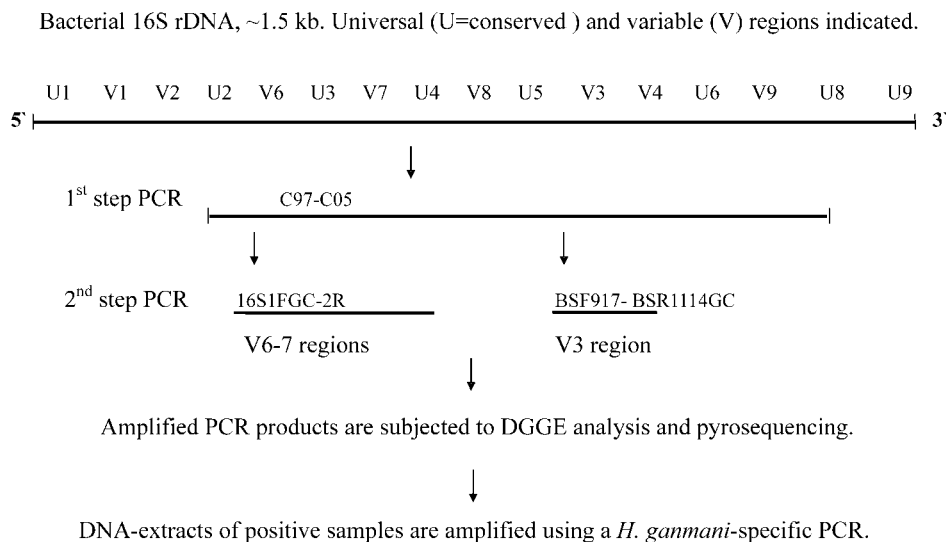Bacterial 16S rDNA, ~1.5 kb. Universal (U=conserved) and variable (V) regions indicated.



FIG. 1. Schematic representation of the strategy used to identify murine *Helicobacter* spp. by multiplex PCR-DGGE, pyrosequencing, and the *H. ganmani*-specific PCR.
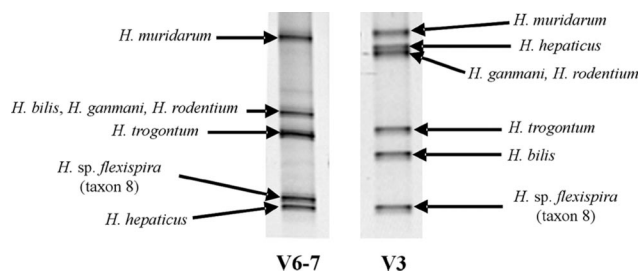
FIG. 2. Migration patterns of V3 and V6-7 regions of 16S rDNA by DGGE analysis of murine *Helicobacter* spp.

the V3 region obtained by pyrosequencing showed 100% similarity of the V3-region sequence to the sequences of the V3 regions of *H. muridarum* and *H. typhlonius*, and because the V6-7 DGGE pattern was different from that for *H. muridarum*, we concluded that these specimens were *H. typhlonius* (Table 2). Sanger sequencing (350 to 385 bp) of the V6-7 regions of 10 such specimens from seven mice confirmed this conclusion (data not shown). In addition, 6 of 29 (20.7%) of specimens from mice in AH-2 had a migration pattern different from those of the reference strains, including *H. trogontum*, whereas DGGE analysis of the V3 region showed a mobility similar to that of the reference *H. trogontum* strain and pyrosequencing of the V3 region demonstrated similarity to *H. trogontum* and a *Helicobacter* sp. flexispira-like organism (Table 2). Sanger sequencing and BLAST analyses of the V6-7 regions of five such specimens showed high degrees of homology to several taxa of *Helicobacter* sp. flexispires. *H. hepaticus* was identified in 23 of 55 (42%) samples from mice in AH-3. All 23 PCR products had DGGE mobilities identical to those of the two *H. hepaticus* reference strains for both the V3 and the V6-7 regions. The sequences of the 23 samples were also 100% similar to that of *H. hepaticus* by pyrosequencing of the V3 region. DGGE of the V6-7 region revealed 27 specimens with mobility patterns similar to those of the reference PCR products of *H. ganmani*, *H. rodentium*, and *H. bilis*. Two of those migrated similarly to the product of *H. bilis* by DGGE of the V3 region, and of the remaining specimens, 20 were positive by the *H. ganmani*-specific PCR (Table 2). Pyrosequencing of the V3 region failed to distinguish *H. ganmani* and *H. rodentium*. Two stomach tissue samples from C3H/HeJ mice, identified as *H. ganmani*-*H. rodentium* by DGGE of the V3 region but negative by the *H. ganmani*-specific PCR, shared high degrees of sequence homology with the sequence of *H. rodentium* by Sanger sequencing of the V6 region.

**Distribution of identified *Helicobacter* spp.** Different patterns of colonization by *Helicobacter* spp. were observed in mice from different animal houses, as shown in Table 3. Mice from AH-1 were colonized mainly with *H. ganmani* and *H. rodentium*, whereas those from AH-2 were colonized with *H. typhlonius* and the *Helicobacter* sp. flexispira-like helicobacter. All species except the *Helicobacter* sp. flexispira-like organism were identified in mice from AH-3. BALB/cA mice from AH-3 were colonized with four *Helicobacter* spp., with *H. hepaticus* as the predominant species. C57BL/6 and C3H mice from AH-3 were frequently positive for *H. typhlonius*, *H. ganmani*, and *H. rodentium*, in contrast to ApoE$^{-/-}$ mice, from which only *H. hepaticus* was identified. As shown in Fig. 3, the

distributions of the different *Helicobacter* spp. in the different mouse specimens were highly variable. *H. hepaticus* and *H. typhlonius* were detected in all tissue types, whereas *H. bilis* was detected in fecal samples only. *H. ganmani* and the *Helicobacter* sp. flexispira-like helicobacter were found in fecal and gastric samples (one blood sample was also positive for the *Helicobacter* sp. flexispira-like helicobacter), and *H. rodentium* was identified in of stomach and small intestine tissue specimens.

**Histologic examination.** Histological changes were observed in 9 of 30 (30%) of the tissue specimens examined, of which 7 were helicobacter positive (Table 4). Except for the liver and the stomach tissue of one IL-10$^{-/-}$ mouse that was helicobacter negative and that showed few abscesses, no changes were observed in tissues negative for *Helicobacter* spp. However, changes were seen in 11 *Helicobacter*-positive specimens. Hepatitis was diagnosed in all the livers of three BALB/cA mice and one ApoE$^{-/-}$ mouse that were positive for a *Helicobacter* sp. identified as *H. hepaticus*. *Helicobacter*-negative livers from the same mouse strains were normal (Table 4). The hepatic inflammation in the affected animals consisted of a few foci of infiltrating polymorphonuclear leukocytes and lymphocytes in various areas of the lobules. The hepatocytes in the foci had increased cytoplasmic basophilia, with a loss of nuclei in some of the cells (Fig. 4A). Kupffer cells appeared to be prominent in one liver, and slight hepatic steatosis was detected in two of the livers. Chronic gastritis and duodenitis were observed in all three C57BL/6 mice cocolonized with *H. typhlonius* and *H. rodentium* or *H. ganmani* (Table 4). The gastritis was characterized by heavy infiltration of polymorphonuclear leukocytes in the basal part of the lamina propria, the submucosa of the corpus, and, to some extent, the adjacent muscular layers (Fig. 4B).

## DISCUSSION

An increasing number of *Helicobacter* spp. are being isolated from a large number of animal species as well as from humans; and some *Helicobacter* spp., such as *H. pullorum* and *H. cinaedi*, infect multiple hosts (8). Hosts, such as rodents and humans, can be colonized with a range of helicobacters, some of which cause or are associated with gastrointestinal disorders. Diagnostic methods such as culture, microscopy, PCR assays, PCR-restriction fragment length polymorphism analysis, and serology have been developed for the detection of murine helicobacters (12, 22, 25, 30). Mahler et al. (17) reported that differentiation of murine *Helicobacter* spp. by colony morphological or histologic features was not possible. Moreover, bacteriological culturing for the detection of *Helicobacter* spp. may require weeks, and isolation can be compromised by the overgrowth of other bacteria. *Helicobacter* sp.-specific PCR assays are limited by the close relatedness of the 16S rDNA and by the large and continuously increasing number of species. PCR-restriction fragment length polymorphism analysis is efficient when it is used with genomic DNA from cultured organisms, but its value is uncertain for the direct detection of *Helicobacter* in animal tissues, in which colonization with more than one *Helicobacter* spp. can occur (13, 27). Consequently, culture-independent methods for the direct detection and identification of species of this genus in biological samples are important.

TABLE 2. Identification of *Helicobacter* spp. in *Helicobacter* genus-positive mouse specimens by multiplex PCR-DGGE, pyrosequencing, and a *H. ganmani*-specific PCR assay

| Animal house[a] | Mouse strain | DGGE result[b] | | Pyrosequencing | *H. ganmani* PCR result[c] | Final identification |
|---|---|---|---|---|---|---|
| | | V6-7 region | V3 region | | | |
| 1 | C57BL/6 (n = 10)[d] | 100% *H. rodentium*, *H. bilis*, *H. ganmani* | 100% *H. ganmani*, *H. rodentium* | 100% *H. ganmani* | 1/10 (−)<br>9/10 (+) | 10% *H. rodentium*<br>90% *H. ganmani* |
| 2 | SPF-SCID (n = 17) | 94% NI[e]<br>6% NI | 94% *H. muridarum*<br>6% *H. trogontum* | 94% *H. typhlonius*, *Helicobacter* sp. flexispira-like organism<br>6% *H. trogontum*, *Helicobacter* sp. flexispira-like organism[f] | | 94% *H. typhlonius*<br>6% *Helicobacter* sp. flexispira-like organism[f] |
| 2 | B6sJl (n = 6) | 83% NI<br>17% NI | 83% *H. trogontum*<br>17% *H. muridarum* | 83% *H. trogontum*, *Helicobacter* sp. flexispira-like organism<br>17% *H. typhlonius* | | 83% *Helicobacter* sp. flexispira-like organism<br>17% *H. typhlonius* |
| 2 | SCID (n = 6) | 83% NI<br>17% NI | 83% *H. muridarum*<br>17% *H. trogontum* | 83% *H. typhlonius*<br>17% *H. bilis*, *H. trogontum*, *Helicobacter* sp. flexispira-like organism | | 83% *H. typhlonius*<br>17% *Helicobacter* sp. flexispira-like organism |
| 3 | C57BL/6 (n = 18) | 44% *H. rodentium*, *H. bilis*, *H. ganmani*<br>56% NI | 44% *H. ganmani*, *H. rodentium*<br>56% *H. muridarum* | 44% *H. ganmani*, *H. rodentium*<br>56% *H. typhlonius* | 1/8 (−), 7/8 (+) | 5% *H. rodentium*<br>39% *H. ganmani*<br>56% *H. typhlonius* |
| 3 | BALB/cA (n = 16) | 73% *H. hepaticus*<br>13% *H. bilis* | 73% *H. hepaticus*<br>13% *H. bilis* | 73% *H. hepaticus*, *Helicobacter* sp. flexispira-like organism<br>13% *H. bilis* | 1/1 (−) | 73% *H. hepaticus*, *Helicobacter* sp. flexispira-like organism[g]<br>13% *H. bilis* |
| 3 | C3H/HeJ (n = 12) | 17% *H. hepaticus*<br>50% *H. rodentium*, *H. bilis*, *H. ganmani*<br>33% NI | 17% *H. hepaticus*<br>50% *H. ganmani*, *H. rodentium*<br>33% *H. muridarum* | 17% *H. hepaticus*, *Helicobacter* sp.<br>50% *H. ganmani*, *H. rodentium*<br>33% *H. typhlonius* | 2/6 (−), 4/6 (+) | 17% *H. hepaticus*<br>33% *H. ganmani*<br>17% *H. rodentium*<br>33% *H. typhlonius* |
| 3 | ApoE−/− (n = 10) | 100% *H. hepaticus* | 100% *H. hepaticus* | 100% *H. hepaticus* | | 100% *H. hepaticus* |

[a] The results for IL-10−/− mice from AH-4 were excluded; hence, all of them were *Helicobacter* negative.

[b] The percentage of *Helicobacter*-specific PCR products with a migration profile identical to that of the indicated reference *Helicobacter* sp. PCR product.

[c] *H. ganmani*-specific PCR was performed with specimens identified as *H. ganmani* or *H. rodentium* by PCR-DGGE and pyrosequencing. The data indicate number of mice positive/total number of mice tested (+, PCR product was detected; −, no PCR product was detected).

[d] *n*, total number of *Helicobacter* sp. detected.

[e] NI, not identified; i.e., the band mobility pattern was different from the patterns for the reference *Helicobacter* strains.

[f] Sanger sequencing of the V6-7 region indicated a *Helicobacter* sp. flexispira-like organism, even though V3 DGGE showed *H. trogontum*.

[g] When the length of the pyrosequence exceeded 43 bases, a high degree of homology was limited to *H. hepaticus*.

TABLE 3. Distribution of *Helicobacter* spp. in *Helicobacter* genus-positive samples from the various mouse strains and animal houses

| *Helicobacter* sp. | No. (%) of *Helicobacter* spp. detected in the indicated mouse strains in the following animal house[a]: | | | | | | | |
|---|---|---|---|---|---|---|---|---|
| | AH-1, C57BL/6 | AH-2 | | | AH-3 | | | |
| | | SPF-SCID | B6sJl | SCID | BALB/cA | C57BL/6 | C3H/HeJ | ApoE−/− |
| *H. bilis* | | | | | 2 (12.5) | | | |
| *H. hepaticus* | | | | | 11 (69) | | 2 (17) | 10 (100) |
| *Helicobacter* sp. flexispira-like organism | | 1 (6) | 5 (83) | 1 (17) | | | | |
| *H. typhlonius* | | 16 (94) | 1 (17) | 5 (83) | 2 (12.5) | 10 (56) | 4 (33) | |
| *H. ganmani* | 9 (90) | | | | | 7 (39) | 4 (33) | |
| *H. rodentium* | 1 (10) | | | | 1 (6) | 1 (5) | 2 (17) | |

[a] The results for IL-10−/− mice from AH-4 were excluded; hence, all of them were *Helicobacter* negative.

Previously, a PCR-DGGE assay targeting the V6-7 region of 16S rDNA was developed for the identification of most *Helicobacter* spp. in the guts of zoo animals, which was based on an optimized *Helicobacter* genus-specific PCR assay with a detection sensitivity of 500 CFU of *H. pylori*/g of spiked feces (1). As this may represent a limiting step, we also included a new region of the 16S rDNA (the V3 region) for the PCR-DGGE analysis used in the present study. The close relatedness of the 16S rDNA among certain species of the genus *Helicobacter* may lead to similar migration profiles by PCR-DGGE; this was observed for reference strains of *H. bilis*, *H. ganmani*, and *H. rodentium* in the analysis of the V6-7 region and in the analysis of the V3 region for *H. ganmani* and *H. rodentium*, as well as for *H. typhlonius* and *H. muridarum*. By contrast, using another set of 16S rDNA-specific primers, Grehan et al. (13) obtained different DGGE profiles for the PCR products, whose sequences were homologous to the *H. ganmani* sequence by DNA sequence analysis. In this study, only one DGGE profile for the PCR products of the *H. ganmani* strains was detected. Optimally, the primers used for PCR-DGGE should be selected so that they amplify conserved regions of different strains within a species but, simultaneously, retain variability to

consistently differentiate organisms at the species level, thereby avoiding interpretation errors leading to misidentification.

PCR-DGGE analysis of both the V3 and the V6-7 regions combined with pyrosequencing allowed identification of most helicobacters, but not *H. ganmani* and *H. rodentium*, as well as a *Helicobacter* sp. flexispira-like helicobacter which possessed a V6-7 mobility pattern different from those of any of the PCR products of the reference strains but similar to that of *H. trogontum* in the V3 analysis. Given the high level of strain-to-strain variation in the 16S rDNA reported for *H. trogontum* and the closely related *Helicobacter* sp. flexispira-like helicobacter strains (14), a definitive identification would not be possible. Distinction of *H. ganmani* and *H. rodentium* required an *H. ganmani*-specific PCR assay. The close relationship of *H. ganmani* and *H. rodentium* has been thoroughly examined previously, and a published PCR assay targeting the 16S rDNA of *H. rodentium* was shown to amplify both species (23). For this reason, we developed a PCR assay for *H. ganmani* that targeted the 16S-23S rDNA internal spacer region but that did not amplify genomic DNA of *H. rodentium* (Tolia et al., submitted).

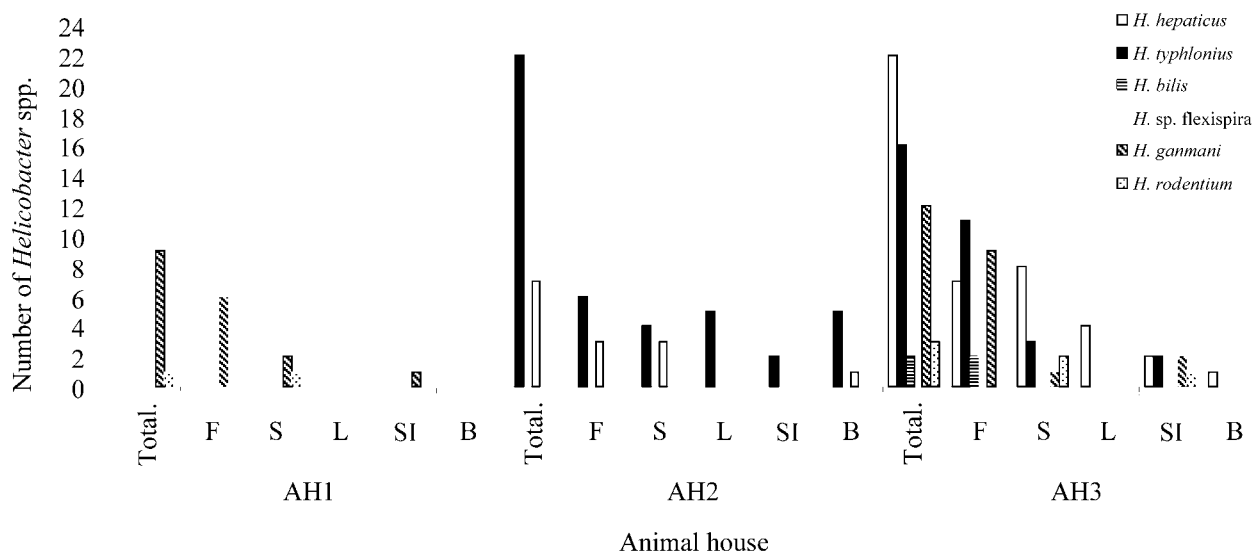Pyrosequencing has been used for the identification of *Hel-*



FIG. 3. Prevalence of *Helicobacter* spp. in different specimens of naturally infected mouse strains from three animal houses (AH-1 to AH-3). Mouse strains shown are C57BL/6 (AH-1); SPF-SCID, B6sJl, and SCID (AH-2); and BALB/cA, C57BL/6, C3H/HeJ, and ApoE−/− (AH-3). The specimens examined were feces (F), stomach tissue (S), liver tissue (L), small intestine tissue (SI), and blood (B).

TABLE 4. Histopathology analysis of specimens (stomach, liver, and small intestine tissue) from mice colonized with *H. hepaticus* or *H. typhlonius*, as well as *Helicobacter*-negative tissue specimens, determined by PCR-DGGE

| AH | Strain | Tissue (no. of specimens) | *Helicobacter* sp. detected | Histo-pathology |
|----|--------|--------------------------|----------------------------|-----------------|
| 2 | SPF-SCID | Liver (4) | *H. typhlonius* | Normal |
| 2 | B6sJl | Liver (1) | *H. typhlonius* | Normal |
| 2 | SPF-SCID | Liver (1) | Negative | Normal |
| 2 | SPF-SCID | Stomach (1) | *H. typhlonius* | Normal |
| 2 | SPF-SCID | Stomach (1) | Negative | Normal |
| 2 | SPF-SCID | Intestine (1) | *H. typhlonius* | Normal |
| 3 | ApoE$^{-/-}$ | Liver (1) | *H. hepaticus* | Hepatitis |
| 3 | ApoE$^{-/-}$ | Liver (2) | Negative | Normal |
| 3 | ApoE$^{-/-}$ | Stomach (1) | *H. hepaticus* | Normal |
| 3 | ApoE$^{-/-}$ | Intestine (1) | Negative | Normal |
| 3 | C57BL/6 | Stomach (3) | *H. typhlonius* | Gastritis |
| 3 | C57BL/6 | Intestine (1) | *H. typhlonius* | Normal |
| 3 | BALB/cA | Liver (3) | *H. hepaticus* | Hepatitis |
| 3 | BALB/cA | Liver (2) | Negative | Normal |
| 3 | BALB/cA | Stomach (5) | *H. hepaticus* | Normal |
| 4 | IL-10$^{-/-}$ | Liver (1) | Negative | Abscess |
| 4 | IL-10$^{-/-}$ | Stomach (1) | Negative | Crypt abscess |

*icobacter* spp. and other bacteria. Pyrosequencing is done by sequencing short segments (25 to 30 nucleotides) of variable 16S rDNA, creating a 16S rDNA signature (15, 18). In the present study, we obtained up to 73 nucleotides (average length, 51 bases; 29 to 73 bases in total) by pyrosequencing of the V3 region of the 16S rDNA. Pyrosequencing alone could not separate closely related murine *Helicobacter* spp., but analyses of the pyrosequences with the BLAST algorithm confirmed the results of the multiplex DGGE analysis.

The isolation of several novel murine helicobacters may call into question the suitability of some laboratory mouse strains as experimental animal models of *H. pylori* infection, especially those involving potential vaccine candidates and other immunological aspects. In addition, past results obtained with a number of experimental murine models in other areas of research should be interpreted with caution. Importantly, exposure to *Helicobacter* spp. antigens prior to experimental infec-

tions may influence the host immune response and, potentially, the results obtained. Furthermore, enteric helicobacters such as *H. hepaticus* and *H. typhlonius* have been shown to cause chronic liver and enteric diseases in susceptible strains of mice (11, 29). Moreover, *H. hepaticus* infection has been shown to be commonly associated with chronic active hepatitis (10) and is widespread among the mice offered by commercial mouse breeders in the United States (24). In the present study, liver specimens of male BALB/cA mice that were positive for *H. hepaticus* by PCR-DGGE were affected by hepatitis (Fig. 4A), whereas BALB/cA livers negative for *Helicobacter* spp. appeared normal. Our findings support previous observations of investigators in the United States (29) and further demonstrate the widespread pathogenic potential of *H. hepaticus* for mice. In addition, *H. typhlonius* has been shown to cause enteric lesions in immunodeficient mice (11), and we observed an acute gastritis associated with *H. typhlonius* colonization in C57BL/6 mice. Although it is possible to deduce that *Helicobacter* spp. are involved in the gastric and hepatic disease development observed in the present study, a disease association does not prove a causal effect, and thus, further studies are required.

Some mice, such as the ApoE$^{-/-}$ strain, were colonized with a single *Helicobacter* sp., whereas all other mouse strains in the same animal house tested were colonized with at least three *Helicobacter* spp., suggesting that host factors influence the susceptibility to colonization with *Helicobacter* spp. Moreover, various degrees of immune deficiency may influence colonization with *Helicobacter* spp., as observed with SCID mice, which displayed the highest prevalence of *Helicobacter* sp. infections. On the other hand, it cannot be excluded that environmental factors, such as food composition, water, and/or fecal contamination, also contribute to differences in *Helicobacter* sp. colonization among the various mouse colonies.

In conclusion, the broad-range diagnostic setup developed in this study was efficient at detecting and identifying most *Helicobacter* spp. colonizing the different parts of the gastrointestinal tracts of laboratory mice. Moreover, we have shown
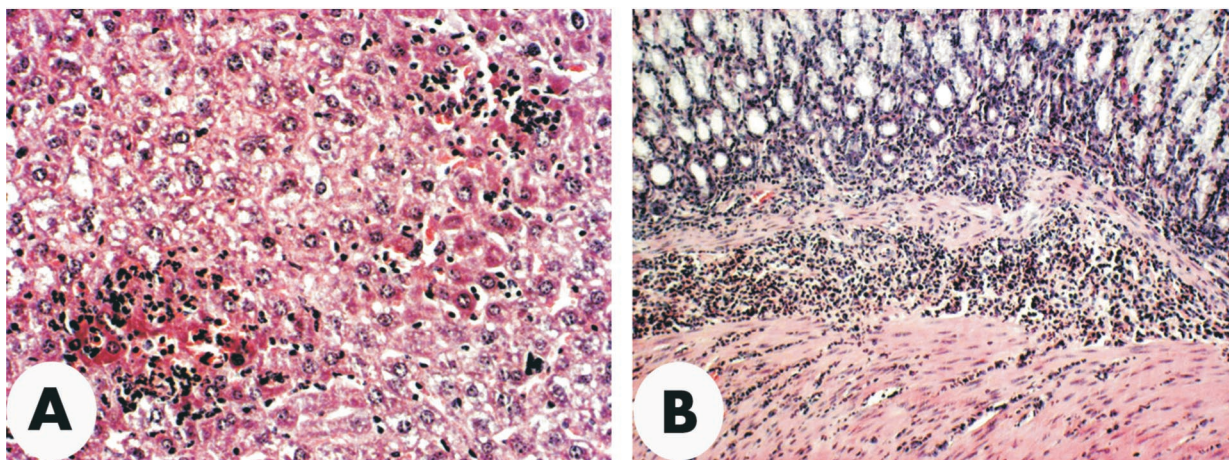
FIG. 4. (A) Hepatitis in a BALB/cA mouse liver characterized by foci of polymorphonuclear leukocytes and lymphocytes. The hepatocytes in these foci had increased basophilia in the cytoplasm and the loss of some of the nuclei. Magnification, ×245. (B) Acute gastritis in C57BL/6 mice showing heavy infiltration by polymorphonuclear leukocytes in the bottom of the lamina propria and in the submucosa, as well as to some extent in the adjacent muscular layers. Magnification, ×125.

an intriguing pattern of murine *Helicobacter* sp. colonization and the association of *Helicobacter* spp. with gastric and hepatic diseases not previously demonstrated in European rodent colonies. The PCR-DGGE approach efficiently detected colonization of a single specimen with multiple species and could prove favorable for the study of this widespread genus and the zoonotic potentials of some helicobacters. It seems likely that other colonies of laboratory rodents also host *Helicobacter* spp. and that more studies should be undertaken to reveal possible routes of transmission, with the ultimate aim of formulating practical guidelines for the creation and maintenance of *Helicobacter*-free rodent colonies.

## REFERENCES

1. **Abu Al-Soud, W., M. Bennedsen, S. L. W. On, I.-S. Ouis, P. Vandamme, H.-O. Nilsson, Å. Ljungh, and T. Wadström.** 2003. Assessment of PCR-DGGE for the identification of diverse *Helicobacter* species, and application to faecal samples from zoo animals to determine helicobacter prevalence. J. Med. Microbiol. **52:**765–771.
2. **Andersen, L. P., S. Kiilerich, G. Pedersen, A. C. Thoreson, F. Jorgensen, J. Rath, N. E. Larsen, O. Borup, K. Krogfelt, J. Scheibel, and S. Rune.** 1998. An analysis of seven different methods to diagnose *Helicobacter pylori* infections. Scand. J. Gastroenterol. **33:**24–30.
3. **Burich, A., R. Hershberg, K. Waggie, W. Zeng, T. Brabb, G. Westrich, J. L. Viney, and L. Maggio-Price.** 2001. *Helicobacter*-induced inflammatory bowel disease in IL-10- and T cell-deficient mice. Am. J. Physiol. Gastrointest. Liver Physiol. **281:**G764–G778.
4. **Clayton, R. A., G. Sutton, P. S. Hinkle, Jr., C. Bult, and C. Fields.** 1995. Intraspecific variation in small-subunit rRNA sequences in GenBank: why single sequences may not adequately represent prokaryotic taxa. Int. J. Syst. Bacteriol. **45:**595–599.
5. **Fox, J., X. Li, L. Yan, R. Cahill, R. Hurley, R. Lewis, and J. Murphy.** 1996. Chronic proliferative hepatitis in A/JCr mice associated with persistent *Helicobacter hepaticus* infection: a model of helicobacter-induced carcinogenesis. Infect. Immun. **64:**1548–1558.
6. **Fox, J., L. Yan, F. Dewhirst, B. Paster, B. Shames, J. Murphy, A. Hayward, J. Belcher, and E. Mendes.** 1995. *Helicobacter bilis* sp. nov., a novel *Helicobacter* species isolated from bile, livers, and intestines of aged, inbred mice. J. Clin. Microbiol. **33:**445–454.
7. **Fox, J., L. Yan, B. Shames, J. Campbell, J. Murphy, and X. Li.** 1996. Persistent hepatitis and enterocolitis in germfree mice infected with *Helicobacter hepaticus.* Infect. Immun. **64:**3673–3681.
8. **Fox, J. G.** 2002. The non-*H. pylori* helicobacters: their expanding role in gastrointestinal and systemic diseases. Gut **50:**273–283.
9. **Fox, J. G., F. E. Dewhirst, Z. Shen, Y. Feng, N. S. Taylor, B. J. Paster, R. L. Ericson, C. N. Lau, P. Correa, J. C. Araya, and I. Roa.** 1998. Hepatic *Helicobacter* species identified in bile and gallbladder tissue from Chileans with chronic cholecystitis. Gastroenterology **114:**755–763.
10. **Fox, J. G., F. E. Dewhirst, J. G. Tully, B. J. Paster, L. Yan, N. S. Taylor, M. J. Collins, Jr., P. L. Gorelick, and J. M. Ward.** 1994. *Helicobacter hepaticus* sp. nov., a microaerophilic bacterium isolated from livers and intestinal mucosal scrapings from mice. J. Clin. Microbiol. **32:**1238–1245.
11. **Franklin, C. L., L. K. Riley, R. S. Livingston, C. S. Beckwith, R. R. Hook, Jr., C. L. Besch-Williford, R. Hunziker, and P. L. Gorelick.** 1999. Enteric lesions in SCID mice infected with "*Helicobacter typhlonicus*" a novel urease-negative *Helicobacter* species. Lab. Anim. Sci. **49:**496–505.
12. **Goto, K., H. Ohashi, A. Takakura, and T. Itoh.** 2000. Current status of helicobacter contamination of laboratory mice, rats, gerbils, and house musk shrews in Japan. Curr. Microbiol. **41:**161–166.
13. **Grehan, M., G. Tamotia, B. Robertson, and H. Mitchell.** 2002. Detection of helicobacter colonization of the murine lower bowel by genus-specific PCR-denaturing gradient gel electrophoresis. Appl. Environ. Microbiol. **68:**5164–5166.
14. **Hänninen, M. L., M. Utriainen, I. Happonen, and F. E. Dewhirst.** 2003. *Helicobacter* sp. flexispira 16S rDNA taxa 1, 4 and 5 and Finnish porcine *Helicobacter* isolates are members of the species *Helicobacter trogontum* (taxon 6). Int. J. Syst. Evol. Microbiol. **53:**425–433.
15. **Jonasson, J., M. Olofsson, and H. J. Monstein.** 2002. Classification, identification and subtyping of bacteria based on pyrosequencing and signature matching of 16S rDNA fragments. APMIS **110:**263–272.
16. **Lee, A., M. Chen, N. Coltro, J. O'Rourke, S. Hazell, P. Hu, and Y. Li.** 1993. Long term infection of the gastric mucosa with Helicobacter species does induce atrophic gastritis in an animal model of *Helicobacter pylori* infection. Zentbl. Bakteriol. Parasitenkd. Infektkrankh. Hyg. Abt. 1 Orig. **280:**38–50.
17. **Mahler, M., H. G. Bedigian, B. L. Burgett, R. J. Bates, M. E. Hogan, and J. P. Sundberg.** 1998. Comparison of four diagnostic methods for detection of *Helicobacter* species in laboratory mice. Lab. Anim. Sci. **48:**85–91.
18. **Monstein, H., S. Nikpour-Badr, and J. Jonasson.** 2001. Rapid molecular identification and subtyping of *Helicobacter pylori* by pyrosequencing of the 16S rDNA variable V1 and V3 regions. FEMS Microbiol. Lett. **199:**103–107.
19. **Muyzer, G.** 1999. DGGE/TGGE a method for identifying genes from natural ecosystems. Curr. Opin. Microbiol. **2:**317–322.
20. **Nedrud, J. G.** 1999. Animal models for gastric *Helicobacter* immunology and vaccine studies. FEMS Immunol. Med. Microbiol. **24:**243–249.
21. **Okazaki, Y., M. Furuno, T. Kasukawa, J. Adachi, H. Bono, S. Kondo, I. Nikaido, N. Osato, R. Saito, H. Suzuki, I. Yamanaka, H. Kiyosawa, K. Yagi, Y. Tomaru, Y. Hasegawa, A. Nogami, C. Schonbach, T. Gojobori, R. Baldarelli, D. P. Hill, C. Bult, D. A. Hume, J. Quackenbush, L. M. Schriml, A. Kanapin, H. Matsuda, S. Batalov, K. W. Beisel, J. A. Blake, D. Bradt, V. Brusic, C. Chothia, L. E. Corbani, S. Cousins, E. Dalla, T. A. Dragani, C. F. Fletcher, A. Forrest, K. S. Frazer, T. Gaasterland, M. Gariboldi, C. Gissi, A. Godzik, J. Gough, S. Grimmond, S. Gustincich, N. Hirokawa, I. J. Jackson, E. D. Jarvis, A. Kanai, H. Kawaji, Y. Kawasawa, R. M. Kedzierski, B. L. King, A. Konagaya, I. V. Kurochkin, Y. Lee, B. Lenhard, P. A. Lyons, D. R. Maglott, L. Maltais, L. Marchionni, L. McKenzie, H. Miki, T. Nagashima, K. Numata, T. Okido, W. J. Pavan, G. Pertea, G. Pesole, N. Petrovsky, R. Pillai, J. U. Pontius, D. Qi, S. Ramachandran, T. Ravasi, J. C. Reed, D. J. Reed, J. Reid, B. Z. Ring, M. Ringwald, A. Sandelin, C. Schneider, C. A. Semple, M. Setou, K. Shimada, R. Sultana, Y. Takenaka, M. S. Taylor, R. D. Teasdale, M. Tomita, R. Verardo, L. Wagner, C. Wahlestedt, Y. Wang, Y. Watanabe, C. Wells, L. G. Wilming, A. Wynshaw-Boris, M. Yanagisawa, et al.** 2002. Analysis of the mouse transcriptome based on functional annotation of 60,770 full-length cDNAs. Nature **420:**563–573.
22. **Riley, L., C. Franklin, R. Hook, Jr., and C. Besch-Williford.** 1996. Identification of murine helicobacters by PCR and restriction enzyme analyses. J. Clin. Microbiol. **34:**942–946.
23. **Robertson, B. R., J. L. O'Rourke, P. Vandamme, S. L. On, and A. Lee.** 2001. *Helicobacter ganmani* sp. nov., a urease-negative anaerobe isolated from the intestines of laboratory mice. Int. J. Syst. Evol. Microbiol. **51:**1881–1889.
24. **Shames, B., J. G. Fox, F. Dewhirst, L. Yan, Z. Shen, and N. S. Taylor.** 1995. Identification of widespread *Helicobacter hepaticus* infection in feces in commercial mouse colonies by culture and PCR assay. J. Clin. Microbiol. **33:**2968–2972.
25. **Shen, Z., Y. Feng, and J. G. Fox.** 2000. Identification of enterohepatic *Helicobacter* species by restriction fragment-length polymorphism analysis of the 16S rRNA gene. Helicobacter **5:**121–128.
26. **Shen, Z., J. G. Fox, F. E. Dewhirst, B. J. Paster, C. J. Foltz, L. Yan, B. Shames, and L. Perry.** 1997. *Helicobacter rodentium* sp. nov., a urease-negative *Helicobacter* species isolated from laboratory mice. Int. J. Syst. Bacteriol. **47:**627–634.
27. **Shomer, N. H., C. A. Dangler, R. P. Marini, and J. G. Fox.** 1998. *Helicobacter bilis/Helicobacter rodentium* co-infection associated with diarrhea in a colony of scid mice. Lab. Anim. Sci. **48:**455–459.
28. **Taneera, J., A. P. Moran, S. O. Hynes, H.-O. Nilsson, W. A. Al-Soud, and T. Wadström.** 2002. Influence of activated charcoal, porcine gastric mucin and β-cyclodextrin on the morphology and growth of intestinal and gastric *Helicobacter* spp. Microbiology **148:**677–684.
28a.**Tolia, V., H.-O. Nilsson, K. Boyer, A. Wuerth, W. Abu Al-Soud, R. Rabah, and T. Wadström.** Helicobacter, in press.
29. **Ward, J. M., J. G. Fox, M. R. Anver, D. C. Haines, C. V. George, M. J. Collins, Jr., P. L. Gorelick, K. Nagashima, M. A. Gonda, R. V. Gilden, et al.** 1994. Chronic active hepatitis and associated liver tumors in mice caused by a persistent bacterial infection with a novel *Helicobacter species.* J. Natl. Cancer Inst. **86:**1222–1227.
30. **Whary, M. T., J. H. Cline, A. E. King, K. M. Hewes, D. Chojnacky, A. Salvarrey, and J. G. Fox.** 2000. Monitoring sentinel mice for *Helicobacter hepaticus, H. rodentium,* and *H. bilis* infection by use of polymerase chain reaction analysis and serologic testing. Comp. Med. **50:**436–443.
31. **Zenner, L.** 1999. Pathology, diagnosis and epidemiology of the rodent *Helicobacter* infection. Comp. Immunol. Microbiol. Infect. Dis. **22:**41–61.